Available online at www.sciencedirect.com
SCIENCE DIRECT
Surface & Coatings Technology 200 (2006) 2870–2874
SURFACE & COATINGS TECHNOLOGY
www.elsevier.com/locate/surfcoat

Characterization of electrodeposited metal coatings by secondary ion mass spectrometry

U. Bardi[a,b], S. Caporali[a,b], S.P. Chenakin[c], A. Lavacchi[a,b], E. Miorin[d], C. Pagura[d], A. Tolstogouzov[a,b,*]

[a]*Dipartimento di Chimica, Università di Firenze, Via della Lastruccia 3, 50019 Sesto Fiorentino, Italy*
[b]*Consorzio Interuniversitario di Scienza e Tecnologia dei Materiali (INSTM) unità di ricerca di Firenze, Via della Lastruccia 3, 50019 Sesto Fiorentino, Italy*
[c]*Institute of Metal Physics, National Acad. Sci. of Ukraine, Blvd. Akad. Vernadsky 36, 03680 Kiev-142, Ukraine*
[d]*Istituto per l'Energetica e le Interfasi (CNR-IENI), Corso Stati Uniti 4, 35127 Padova, Italy*

Received 15 July 2004; accepted in revised form 19 November 2004
Available online 5 January 2005

Abstract

This paper reports the results of the elemental identification and depth profiling by secondary ion mass spectrometry (SIMS) of electroplated Ru, Pd and Au coatings on a brass substrate precoated with a nickel layer. The measurements were performed by a low-cost, custom-built instrument based on standard commercial components. The secondary ion species were identified using DECO computer code. X-ray photoelectron spectroscopy (XPS) was applied for complementary surface elemental analysis of the samples. The sputter-produced crater was measured by a stylus profiler, and the nondestructive estimation of the nickel underlayer thickness was carried out by energy dispersive X-ray fluorescence analysis (EDXRFA). It is shown that thickness of the Ru film is ca. 2.6 μm, and for the Pd and Au coatings its number lies within the range of 0.4–0.5 μm. The experimental data indicate that the Ru film contains only a few percents of nickel, and the Ru–Ni interface, in contrast with the Pd–Ni and Au–Ni interlayer boundaries, appears to be sharp due to low mutual solubility in the Ni–Ru system. On the contrary, the Pd coating can be considered as a Ni–Pd alloy with Ni concentration amounting up to 90 at.% by the SIMS and XPS estimation. The appreciable content of Ni (ca. 35–40 at.%) is revealed on the surface of the Au film by XPS. For the Ru coating, the thickness of the Ni underlayer estimated by EDXRFA is 12.2 μm; the evaluated thickness of the Ni substrate for the Pd and Au coatings is about 4.5 μm and less than 1 μm, respectively, and it can be taken only as "apparent" values because of formation of solid solutions in these systems.

PACS: 68.55.Nq; 82.80.Ms
Keywords: Secondary ion mass spectrometry (SIMS); Electroplating; Gold; Palladium; Ruthenium; Depth profiling

1. Introduction

The electrodeposition or electroplating of metal coatings (e.g., gold, palladium or ruthenium films) is a well-established method utilized in the industry for protective and decorative purposes. Although electrodeposition is considered to be a mature technology, its optimization remains a goal worth pursuing with the purpose of obtaining high-quality coatings and, in general, saving resources and expensive materials.

The optimization of metal electroplating should start from an accurate characterization of the coatings. Normally, their thickness is of the order of one-tenth of a micrometer. Such a thickness is, in principle, within the resolution of scanning electron microscopy (SEM), however, the sample preparation for this technique is far from being routine and the spatial resolution of energy dispersed X-ray analysis is normally not sufficient to perform an elemental analysis of coatings.

* Corresponding author. Dipartimento di Chimica, Università di Firenze, Via della Lastruccia 3, 50019 Sesto Fiorentino, Italy. Tel.: +39 055 457 3116; fax: +39 055 457 3120.
E-mail address: alexander.tolstoguzov@unifi.it (A. Tolstogouzov).

0257-8972/$ - see front matter © 2004 Elsevier B.V. All rights reserved.
doi:10.1016/j.surfcoat.2004.11.029

In the present work, we describe how secondary ion mass spectrometry (SIMS) can be used to determine thickness and composition of electroplated metal layers. SIMS has proved to be a sensitive tool for trace elemental, sputter depth profiling and chemical imaging (mapping) analyses of any solid materials (see, e.g., Refs. [1,2] and references cited therein). This technique measures the atomic and molecular ion emission (*secondary ions*) produced by energetic ion impact (*primary ions*). So far, SIMS has been widely used in the semiconductor and microelectronics industries because of the extreme detection limit and depth resolution possible. The problem raised here is that SIMS typically involves large, complex and expensive equipment, and the cost of analysis restricts its use to a few situations where the expense can be justified. Our purpose was twofold: first, to examine the applicability of a reasonably priced custom-built SIMS instrument for thorough characterization of commercial electroplated metal layers, and secondly, as a consequence, to explore the possibility of using SIMS as a routine characterization method, requiring less effort in a sample preparation than conventional electron microscopy.

Here, we report the results of SIMS elemental identification and depth profiling of Ru, Pd and Au coatings with appropriate calibration of the sputter depth by a stylus profiler and nondestructive estimation of the nickel sublayer thickness by energy dispersive X-ray fluorescence analysis (EDXRFA). Additional surface elemental analysis of the samples was carried out by X-ray photoelectron spectroscopy (XPS) [2].

2. Experimental

The coatings examined in the present work were commercially produced Ru, Pd and Au films on a Ni-coated brass. They were fabricated according to the conventional electroplating technology [3,4], however, the details of the process and composition of the galvanic bath are proprietary know-how. No postdeposition treatments of the films were performed, except for rinsing in ethanol before introduction into the analytical chamber.

SIMS measurements were carried out by means of a dedicated instrument based on standard commercial components. Details of the system have been reported in previous publications [5–7]. Briefly, a duoplasmatron ion gun (model DP50B by VG Fison) generates mass-filtered $^{16}O_2^+$ primary ions with a bombarding energy of 6 keV. The ion current density was (0.1–0.2) mA/cm^2, and the raster-scanned primary beam sputtered a target area of about 0.25 mm^2. Positively and negatively charged secondary ions were measured by a Hiden EQS 1000 mass energy analyser [8]. This instrument unifies a high transmission electrostatic energy analyser and a quadrupole mass-spectrometer with mass resolution ΔM (FWHM)=0.75±0.05 amu in the mass interval of 1–1000 m/z. The analysed zone of the crater created by ion bombardment was limited to 20% by means of electronic gating of the registration system. The operating pressure in the analytical chamber was $(1–2)\times10^{-8}$ mbar. The residual gas atmosphere was monitored by the same Hiden EQS 1000 Analyser.

The depth of the sputtered craters was determined by a Tencor Stylus Profiler P-10. We used a Fischerscope XAN X-ray fluorescence analyser [9] to estimate the Ni-underlayer thickness (without sputtering of the coatings). XPS analysis was performed by a standard spectrometer equipped with a hemispherical electron energy analyser and an Al-Kα X-ray source.

3. Results and discussion

A typical mass spectrum of the positive secondary ions measured during sputter depth profiling of the Ru coating is shown in Fig. 1. The statistical variation between three measurements performed in three different points of the sample was within ±20%. The spectrum appears very complex. It includes mass peaks of (i) atomic ions of the coating material and impurities, (ii) surface and bulk contaminant species and (iii) oxygen- and hydrogen-containing molecular ions.

The generation of different molecular (cluster) secondary ions by oxygen ion-beam bombardment, particularly under dynamic sputtering conditions, is a complex process (see Refs. [1,2]), and such ions cannot be used directly for the chemical identification of surface compounds. Molecular peaks can coincide in mass number (m/z) with atomic peaks and such superposition makes identification of ion species rather difficult. The problem is especially important for quadrupole-based SIMS, which does not provide the same high mass resolution as more expensive and complicated magnetic and time-of-flight analysers do. Using quadrupole

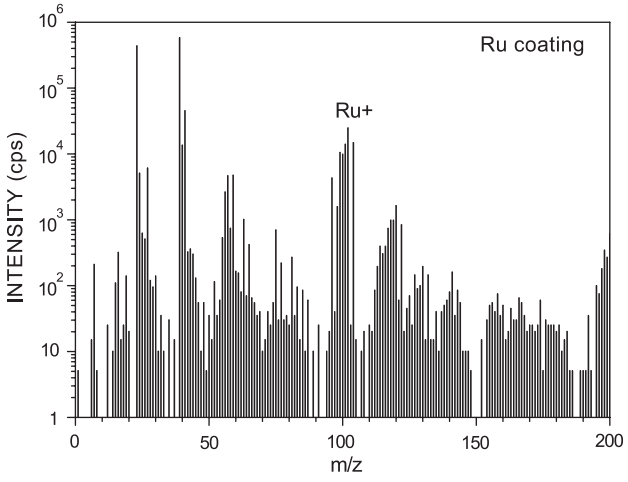

Fig. 1. Mass spectrum of the positive secondary ions measured upon sputtering of the Ru coating. Experimental conditions: $^{16}O_2^+$ primary ions, E_0=6 keV, I_0=250 nA, raster 0.5×0.5 mm^2, 20% electronic gating. Results of the ion species identification are presented in Table 1.

Table 1
Identification of the positively charged secondary ions emitted from the Ru coating (Fig. 1)

Ion species	Intensity ($\times 10^3$ cps)
K	526
Na	436
Ru	80
Ca	14
Al	6.1
CaH	5.6
Mg	5.3
KH_2	4.5
$RuOH_2$	4.4
CaO	1.7
RuO	1.4
Cu	1.3
Fe	1.1
NaH	0.92
Ni	0.75
NiH	0.42
RuOH	0.41
O	0.32
CaH_2	0.25
Mn	0.24
Li	0.23
Au	0.18
Zn	0.17
Cr	0.15
Si	0.14
Ni_2	0.1

Sum total of the peak intensities is 1.092×10^6 cps, and the unidentified remainder is 5.1×10^3 cps (0.5%).

mass-analysers, the decomposition and the interpretation of complex mass spectra are generally based on the assumption that peak intensities correspond to native isotope abundance of the given element [10,11]. In this study, we used DECO computer code [12] for spectra identification. An operator takes an active part in the process of spectra decomposition by this program, specifying and correcting the list of ion species and trying to improve the quality of interpretation by minimizing the undefined remainder of the sum total of the peak intensities.

Table 1 shows the results of the ion species identification for the Ru coating (Fig. 1). The intensities reported in this table are the sum of all isotope ions for every species. The high intensities of the alkali and alkaline-earth metal ions result from their ultrahigh positive ion yields (ionization probabilities). The mass spectrum of the Pd coating is not shown here. We only point to a large number and high intensity of the hydrogen-containing ions sputtered from this sample due to the tendency of palladium to absorb hydrogen.

For the Au coating, we measured negatively charged secondary ions (Fig. 2) since Au exhibits a small positive ion yield. The results of the identification are summed up in Table 2. The dominant compounds here are hydrocarbons, halogens, halogen- and oxygen-containing species characterized by the first-rate capability to be emitted as negatively charged secondary ions.

The SIMS depth profiling data are shown in Fig. 3(a–c). The profiles represent the major isotope ions of the coating materials ($^{102}Ru^+$, $^{106}Pd^+$ and $^{197}Au^-$), $^{58}Ni^+$ and $(^{58}Ni^{16}O_2)^-$ ions for the underlayer, and the most intense ions of contaminants (Na^+ or Cl^-). In spite of the fact that the Na^+ peak intensity is very high throughout the depth of the coatings, particularly, for the Ru film (Fig. 3a), the atomic concentration of sodium does not exceed 0.5–1% according to our estimation based on the elemental sensitivity factors from Ref. [13]. It appears that contamination of the galvanic bath is responsible for such a level of impurity content. However, we have no available information how this contamination influences the quality of the coatings.

The depth scale in Fig. 3 was derived from the total depth of sputter crater Z, which was determined by a stylus profiler after ending of the sputtering, assuming that the erosion rate is $V_{sp}=dz/dt\sim Z/T$, where T is the time of sputtering. This supposition is not completely correct for the samples consisting of several layers with different sputtering coefficients. However, in our case, such difference is small enough, and the worst inaccuracy in the sputter rate does not exceed 20–25%. By means of this procedure, we estimated the erosion rate to be 33 ± 5 nm/min for Ru coating, 50 ± 10 nm/min for Pd and 60 ± 12 nm/min for Au coatings. The thickness of the coatings calculated at the level of 0.5 I_{max} of the corresponding signals are presented in Table 3.

As can be seen from Fig. 3a, the ruthenium coating is rather pure and contains only a few atomic percents of nickel, which penetrates the coating. It is also contaminated by sodium, which is homogeneously distributed in the Ru film with a concentration being somewhat larger than that in the underlying Ni layer. Note that in comparison with the Pd–Ni and Au–Ni interlayer boundaries the Ru–Ni inter-

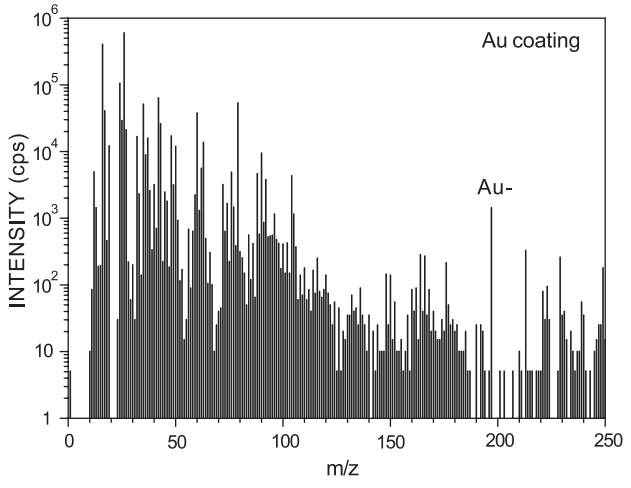

Fig. 2. Mass spectrum of negative secondary ions obtained upon sputtering of the Au coating. Experimental conditions: $^{16}O_2^+$ primary ions, E_0=6 keV, I_0=250 nA, raster 0.5×0.5 mm^2, 20% electronic gating. Results of the ion species identification are presented in Table 2.

Table 2
Identification of the negatively charged secondary ions emitted from the Au coating (Fig. 2)

Ion species	Intensity ($\times 10^3$ cps)
C_2H_2	616
O	405
C_2	108
Cl	67
C_2H_2O	65
CH_3O_4	53
OH	41
$C_2H_4O_2$	39
C_2H	27
C_2H_3O	24
C4	18
O2	17
CH_3O_3	14
C_4H_2	13
F	12
HCl	11.5
NiO_2	10.5
H_2Cl_2O	7.9
H_2Cl_2	5.1
C	5
C_2O	3.3
$NiOH_2$	3
HO_3	2.4
HO_2	2.3
$C_2H_3O_2$	2.3
$NiOH_3$	2
$H_2Cl_2O_2$	1.9
CH_2O_2	1.85
$C_2H_2Cl_2$	1.6
Au	1.43
CH	1.4
NiCl	1.1
Ni	0.98
Cl_2O_2	0.98
Cl_2H_3	0.84
ClO	0.47
AuO	0.33
CH_2	0.18
CO	0.14
COH	0.06

Sum total of the peak intensities is 1.616×10^6 cps, and the unidentified remainder is 26.6×10^3 cps (1.6%).

face appears to be sharp that may be explained by a negligible mutual solubility in the Ni–Ru system at low temperatures [14,15].

On the contrary, the experimental data indicate that Pd coating is not single component; it contains a great amount of Ni and Na contamination as well, with Na accumulating at the coating surface (Fig. 3b). This result can be interpreted assuming that the Pd film is not continuous or that a Ni–Pd alloy with high concentration of Ni is formed during the coating deposition or afterwards. The second hypothesis looks more plausible because of these elements tend to form continuous solid solutions in the whole range of concentrations [16]. For the sample studied, the nickel content in the alloy may amount up to 90 at.% on the basis of the SIMS elemental sensitivity factors [13]. The XPS

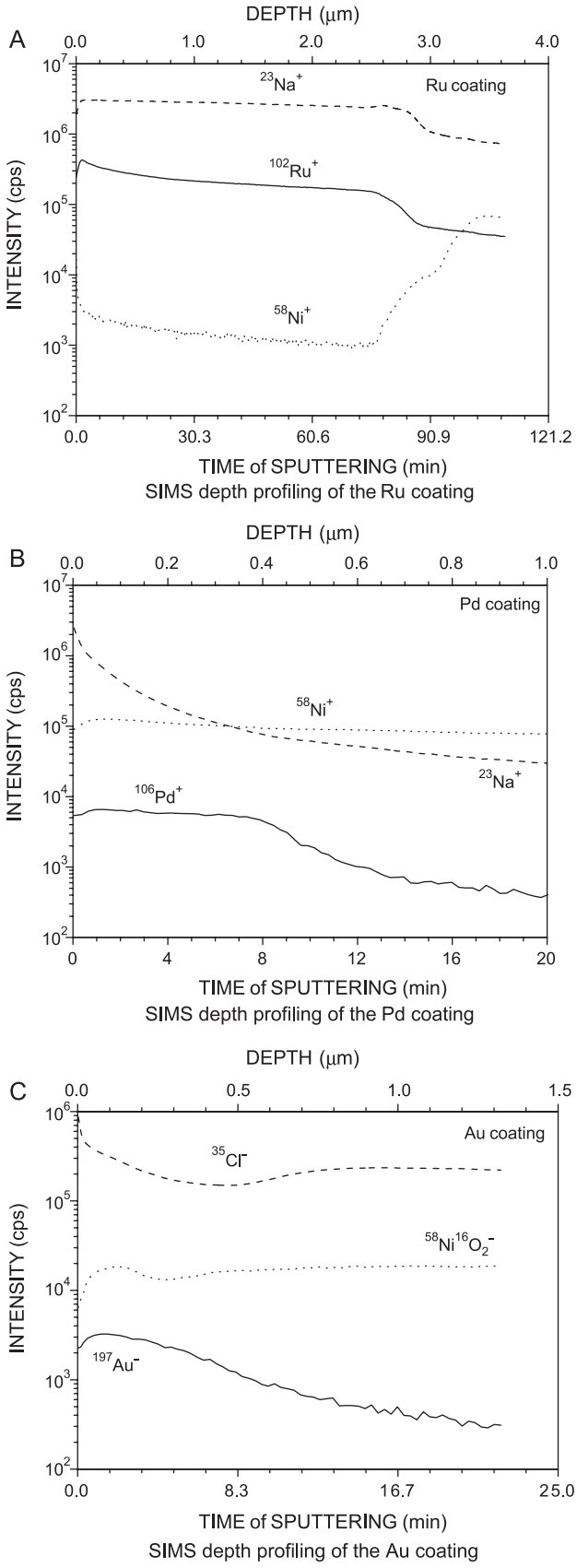

Fig. 3. SIMS depth profiling of Ru (A) and Pd (B) coatings using positive secondary ions, and of Au (C) coating using negative secondary ions.

Table 3
Characteristics of the samples determined by SIMS and by X-ray fluorescence technique

Coating	Thickness (μm)	Main impurities	EDXRFA estimation of the Ni underlayer thickness (μm)
Ru	2.6±0.4	Cu, Au, Fe, Zn, Cr	12.23±0.09
Pd (+Ni)	0.45±0.09	Cu, Pt, Os, Zn, Ru, Fe, Cr	4.5
Au (+Ni)	0.42±0.08	Cu, Ag, Zn, Fe, Cr	<1

measurements also reveal heightened Ni content in the near-surface layer, approximately of the same magnitude.

In the Au–Ni system, mutual solubility and formation of continuous solid solutions takes place at high temperature (more than 800 °C). However, at low temperatures a miscibility gap arises and equilibrium solubility of Au in Ni (and vice versa) becomes very low [17,18]. Nevertheless, our results demonstrate that the gold coating also contains an appreciable amount of Ni, and the interlayer boundary is smeared (Fig. 3c). According to XPS data, the concentration of nickel on the sample surface is about 35–40 at.%. Ni layer, in fact, is used as a "diffusion barrier" to prevent penetration of the components of brass, particularly copper, into the Au plating. However, our data evidence the possibility of Ni diffusion into the coating to form a solid solution, and structural defects arising during electroplating of Au could promote such process. This result is in agreement with the data reported in Ref. [19].

The thickness of the Ni underlayer was determined for each sample in 6 different points by means of non-destructive X-ray fluorescence. The data are presented in Table 3. In estimating the uncertainty of these data, we remark that Fischerscope XAN analyser calculates the thickness of "buried" metal layers rested upon a simple model of well-defined interlayer boundaries. In our study, such assertion is completely correct only for Ru coating. For Pd and Au coatings, which tend forming solid solutions with nickel, the evaluated thickness of the Ni underlayer listed in Table 3 has to be considered only as an "apparent" value.

4. Summary

Sputter depth profiling by SIMS is an effective method for the characterization of electrodeposited metal coatings. The results of the present work show that it is possible to use the method to obtain such data as layer thickness, purity and composition, and in particular to study the formation of alloys in the coatings. The presence of interfacial contamination can also be accurately determined. The method is quick; typically 20–25 min are required for a complete depth profiling to a depth of 1 μm. The most interesting characteristic of SIMS lies perhaps in the fact that it requires no special sample preparation beyond simple cleaning. In this respect, the method turns out to be much more practical than SEM, where sample preparation is complex and critical for this range of thicknesses. It is important that our measurements were performed using a custom-built SIMS installation with moderate cost of the analysis.

The coupling of SIMS and EDXRFA is useful for characterization not only of coatings but of underlayers as well, with some limitation for the systems forming solid solutions. SIMS imaging [20] is a very promising technique to control spatial homogeneity of electrodeposited films, and it will be object of further investigations.

References

[1] A. Benninghoven, F.G. Rüdenauer, H.W. Werner, Secondary Ion Mass Spectrometry, Wiley, New York, 1989.
[2] J.C. Riviere, S. Myhra (Eds.), Handbook of Surface and Interface Analysis, Marcel Dekker, New York, 1998.
[3] E. Bertorelle, Trattato di Galvanotecnica, vol. 1, Ulderico Hoepli, Milano, 1972 (in Italian).
[4] M. Schlesinger, M. Paunovic, Modern Electroplating, Wiley, New York, 2000.
[5] A. Tolstogouzov, S. Daolio, C. Pagura, Surf. Sci. 441 (1999) 213.
[6] A. Tolstogouzov, S. Daolio, C. Pagura, Nucl. Instrum. Methods, B 183 (2001) 116.
[7] A. Tolstogouzov, S. Daolio, C. Pagura, C.L. Greenwood, Int. J. Mass Spectrom. 214 (2002) 327.
[8] Hiden Analytical, 420 Europe Boulevard, Warrington WA5 7UN, England.
[9] Helmut Fischer GmbH+Co.KG, 71069 Sindelfingen, Germany.
[10] W. Steiger, F.G. Ruedenauer, J. Antal, S. Kugler, Vacuum 33 (1983) 321.
[11] A. Tolstogouzov, Eur. Microsc. Anal. 3 (1997) 17.
[12] E. Laptev, unpublished data.
[13] R.C. Wilson, Int. J. Mass Spectrom. 143 (1995) 43.
[14] R.P. Elliott, Constitution of Binary Alloys, First Supplement, vol. 2, McGraw-Hill Book, New York, 1965.
[15] F.A. Shunk, Constitution of Binary Alloys, Second Supplement, McGraw-Hill Book, New York, 1969.
[16] M. Hansen, K. Anderko, Constitution of Binary Alloys, vol. 2, McGraw-Hill Book, New York, 1958.
[17] M. Hansen, K. Anderko, Constitution of Binary Alloys, vol. 1, McGraw-Hill Book, New York, 1958.
[18] H.G. Tompkins, M.R. Pinnel, J. Appl. Phys. 48 (1977) 3144.
[19] A.S. Kuz'min, Yu.I. Surov, V.A. Maksimova, G.M. Kosova, Zashch. Met. 12 (1976) 480 (in Russian).
[20] A. Lamperti, C.E. Bottani, P.M. Ossi, R. Levi-Setti, Surf. Coat. Technol. 180–181 (2004) 323.